Elaboration and characterization of cross-linked (Tripropylene glycol diacrylate)/modified Montmorillonite-M^+ nanocomposites

Ahmed Benamor[1,2], Yazid Derouiche[3], Ameur Ouali[1,2], Lahcene Souli[4], Riadh Bourzzami[5], Ulrich Maschke[6]

[1]Physics Department, Faculty of Science, University of M'sila, 28000 M'sila, Algeria
[2]Laboratory of Physics, Physics Department, Faculty of Science, University of M'sila, 28000 M'sila, Algeria
[3]Physico-Chemical Laboratory of Materials and Environment, ZianeAchour University of Djelfa, Djelfa 17000, Algeria.
[4]Laboratory of Organic Chemistry and Natural Substances, Department of Chemistry, Faculty of Exact Sciences and Informatics, ZianeAchour University of Djelfa, Djelfa 17000, Algeria
[5]Emerged material unit, Setif University, Setif, Algeria
[6]Materials and Transformations Unit (UMET), UMR 8207–CNRS, Building C6, University of Lille Sciences and Technologies, 59655 Villeneuve d'AscqCedex, France

Email corresponding author :ahmed.benamour@univ-msila.dz

Received: 05/ 2023; Accepted: 06/ 2023; Published: 07/ 2023

Abstract
In this work, Tripropylene Glycol Diacrylate (TPGDA)/Montmorillonitenanocomposites were elaborated via in-situ physical cross-linking of TPGDA method with different type of cationically exchanged montmorillonite (MMt-M^+; M = K, Na, Li). In addition, the cationic exchange of the Montmorillonite clay is carried out using the chemical products KCl, NaCl and LiCl as source of the cations K^+, Na^+, Li^+ respectively**.** The synthesized cross-linked **(**TPGDA/MMt-M^+) nanocomposites were characterized by Fourier Transform Infrared Spectrum (FTIR), X-ray diffraction (XRD), Scanning Electron Microscopy (SEM) and Thermogravimetric analysis (TGA).Based on the DTG curve, the activation energy and kinetics parameters of the decomposition phase were calculated for each sample using the Coats and Redfern model.

Keywords: Nanocomposites, Montmorillonite, TPGDA.PotassiumPeroxydisulfate.
DOI Number: 10.48047/nq.2023.21.6.NQ23143 **NeuroQuantology2023;21(6): 1404-1415**

1. INTRODUCTION

Silicate-based nanocomposite materials have attracted a great deal of interest in the academic and industrial world as they show a remarkable improvement in the properties of materials over pure polymers or conventional micros and macro-composites.These improvements may include high modulus,increased heat resistance, decreased gas permeability, flammability and increased biodegradability of polymers.The changing into higher properties depends on a certain number of parameters such as the distribution of the clay (dimensions, form factor, exfoliation...) and the reinforcement-polymer interaction(Picard et al., 2007;Ogasawara et al., 2006).

Although the intercalation chemistry of polymers when blended with suitable silicate layers has been known for a long time, the field of polymer-based nanocomposites has recently increased.

A composite is a hetero-phase material consisting of an assembly of at least two immiscible phases (Sheldon, 1982). The combination of these two phases is sought in such a way as to lead to a al.,1998) properties, and thus broadening their field of application.

Bentonite is one of the clay minerals –hydrated Aluminum silicate. The major component in bentonite is montmorillonite which belongs to the group of silicate minerals known as dioctahedralsmectites. Structure of this kind of materials is formed by two tetrahedral layers sandwiching an octahedral layer. The tetrahedral sites are occupied by Si(IV) as a central atom while the octahedral ones contain Al(III) which can be substituted with Fe(III) or/and Mg(II).This kind of structure exhibits cationic exchange properties and swelling ability(Madejová et al., 1999; Tyagi et al., 2006; Kubranová et al, 2003; Radojevic et al, 2007).

TPGDA is a macromolecule contains double bends in its chemical structure (Fig.1). It's an important feedstock for chemical syntheses because it reasily enters into addition reactions.

synergy of properties that could not be induced individually. These materials are made up of a matrix and reinforcement. The matrix can be made of a metallic, ceramic or polymeric material (Sheldon, 1982).The reinforcement ensures the mechanical strength of the matrix and can be in the form of particles or fibers. Composite materials can provide many functional advantages: lightness, mechanical and chemical resistance, better thermal and chemical resistance and electrical insulation(Alexandre, 2000).

Many studies have shown the advantage of incorporating nano-fillers in polymeric materials. Indeed, the addition of a small amount of nano-charge makes it possible to improve their mechanical (Okada,1995; Reynaud et al., 2001; Yang 2004), thermal (Gilman, 1999; Wang et al.,2004, electrical (Wan, 1998; Zheng et al., 2002)or magnetic (Barnakov et al.,2004; Wan et

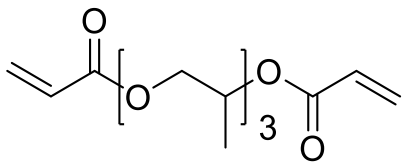

Fig. 1 Chemical structure of Tripropylene glycol diacrylate (TPGDA).

montmorillonite.The nanoparticles obtained under optimal conditions were characterized from a structural and thermal point of view. The second objective is to use the modified TPGDA as reinforcing filler in a montmorillonite matrix and to explore the structural, thermal properties of nanocomposites. The strategy of the work is based on intercalation the monomer into the solution polymerization process.

2. EXPERIMENTATION

Materials

Tripropylene glycol diacrylate (TPGDA**)** (Sigma-Aldrich) was used as received. The bentonite clay used in this study is montmorillonite clay was produced from an Algerian society of bentonite (BENTAL). All our experiments were carried out on the same batch of the bentonite. KCl, NaCl and LiCl(Sigma-Aldrich) were used as received, potassium peroxydisulfate (Sigma Aldrich).

Preparation of exchanged montmorillonite-M^+ (M^+ = K, Na, Li)

The polymerizable groups allow the product to be used as a cross-linking component, in radiation-curing coatings, where it also acts as a thinner. The product can be polymerized by the usual bulk, solution, suspension and emulsion techniques. When the stabilizer is removed of before, it is generally unnecessary as its effect can be counteracted by an excess of initiator.

Bulk polymerization is one of the most efficient processes for the production of inorganic-organic nanocomposites. In this case, the preparation of these materials consists of the bulk polymerization of a monomer by the radical way in the presence of nano-sized mineral particles. The properties of the new material depend strongly on the interfacial interactions between the two phases brought into contact in the synthesis domain. A great deal of work has been carried out on bulk polymerization in the presence of particles of very varied natures.

The first objective of this work is therefore to carry out a physicochemical and mineralogical characterization of this clay in order to optimize the process of organophilization of

Characterization

FT-IR spectrums were obtained by Nicolet Avatar 330FT-IR Fourier Transform Interferometer over a range of 400 to 4000 cm^{-1} with a resolution of $2cm^{-1}$. X-ray diffraction analysis were obtained using X-ray diffractometer (PW-1710, Philips) with a Cu-Kα(λ= 1.54 Å) in the 2θ between (range:3–65°). Cross-linked (TPGDA/MMt-M^+) nanocomposites images were observed by scanning electron microscope SEM, type (Japanese Neoscope JCM-5000). Thermals analysis ATG was carried out by "SETARAM Labsys" type device. The curves are recorded between 25 and 900˚C, with a rate of 10˚C/min.

3. RESULTS AND DISCUSSION

X-ray diffraction analysis

X-ray analysis of the treated montmorillonite, cross-linked (TPGDA)/MMt-Li^+, cross-linked (TPGDA)/MMt-Na^+ and cross-linked (TPGD)/MMt-K^+ are presented in the Fig.2 (a, b, c and d) respectively.

A mass of 30g of the fine bentonitepowder was mixed with 1 liter of distilled water and 30 ml of hydrogen peroxide. The heterogeneous mixture was stirred for 2 hours at room temperature and then centrifuged for 20 minutes at 6000 rpm. The montmorillonite then was dried at 80˚C for overnight. Then 10g of crude clay was mixed with (500ml, 1N) of MCl (M = Li, Na, K), the suspension was stirred for 4 hours, then centrifuged for 15 minutes at 9000 rpm. This operation is repeated three times. The cationic exchanged montmorillonite was dried at 80˚C (Haouzi, 2004).

Synthesis of cross-linked (Tripropylene glycol diacrylate)/Montmorillonitenanocomposites

A mass of 5.21g of TPGDA was mixed with 0.5g of montmorillonite in a round bottom flask. The mixture was heated at 80˚C with continued stirring about 120h. After 5 days the initiator potassium peroxydisulfate was added, the mixture is heated at 80°C for 3 hours under reflux. Finally, the nanocomposite was then dried under vacuum.

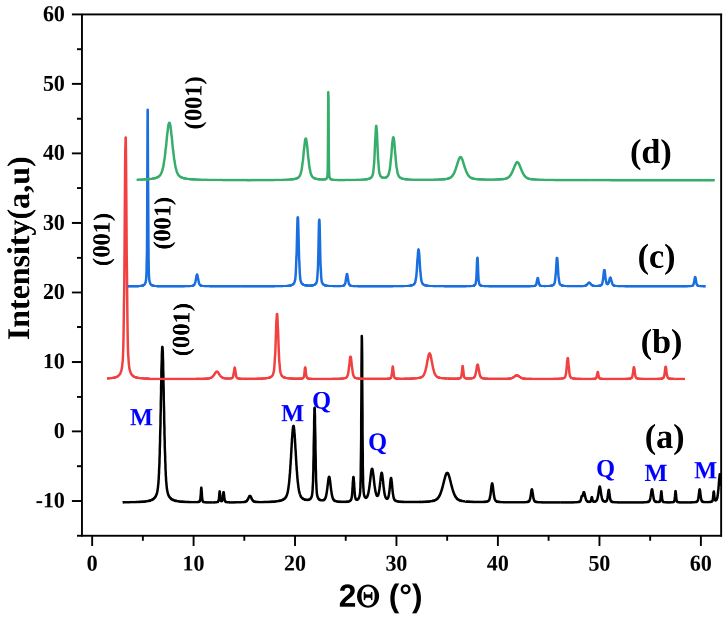

Fig. 2X-raydiffractograms of: (a) MMt-Na^+, (b) cross-linked (TPGDA)/MMt-Li^+ nanocomposite, (c) cross-linked (TPGDA)/MMt-Na^+ nanocompositeand (d) cross-linked (TPGDA)/MMt-K^+ nanocomposite. (M) refers to montmorillonite; (Q) refers to quartz.

Firstly, the analysis clearly shows that the cross-linked (TPGDA) was interposed between the montmorillonite-M^+ layers by forming nanocomposite materials. There is a big difference between the spacing of nanocompositescross-linked (TPGDA)/MMt-Li^+, cross-linked (TPGDA)/MMt-Na^+ and cross-linked

(TPGDA)/MMt-K^+. The Fig.3 is used to calculate the value of the basic spacing d_{001} in the sample nanocomposites. The values obtained are ordered as follows:
d_{001}(cross-linked(TPGDA)/MMt-Li^+)>d_{001}(cross-linked(TPGDA)/MMt-Na^+)>d_{001}(cross-linked (TPGDA)/MMt-K^+).

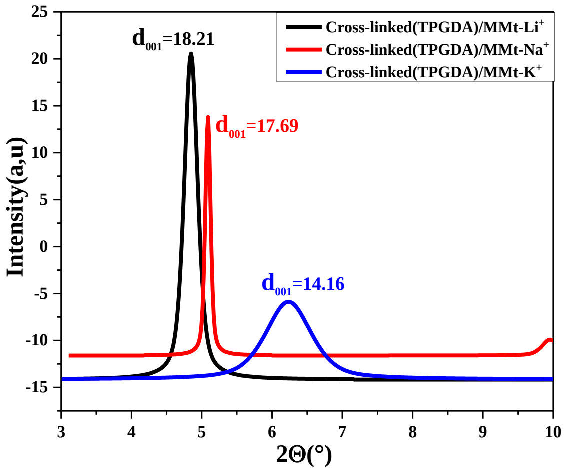

Fig. 3 Comparison of the positions of (001) reflection peaks of cross-linked (TPGDA)/MMt-M^+ nanocompositesamples

Small cations (Li^+ and Na^+ for alkaline compensating cations) can easily be inserted into the hexagonal cavity, while the K^+cation follow the inhibitory potential (Berend,1991). Table (1) summarizes the offset of the difference of the base spacing (d_{001}). 1407

Table 1. Interlayer distance for cross-linked (TPGDA)/MMt-M^+ nanocomposite and ionic radius of the cations.

Sample	Li^+	Na^+	K^+
d_{001}(Å) cross-linked(TPGDA)/MMt-M^+ Ionic radius (Å)	18.08 0.6	17.69 0.95	14.16 1.33

of the Si-O-Si bond(dos Santos et al.,2015). In addition, the division of the OH group between the atoms Fe, Al and Mg in the octahedral position can shift the vibrations Al-OH towards the low frequencies around 815and 915 cm^{-1}. 914.2 cm^{-1} corresponds to Al-Al-OH (Sposito et al., 1983). 848.6 cm^{-1} corresponds to Al-Mg-OH (dos Santos et al., 2015). The weak band 796 cm^{-1} is attributed to the vibrations of quartz. The bands 514, 465 and 425 cm^{-1}arecorresponded of Si-O-Al deformation vibration (Wu et al., 2009). We also note on the FT-IR spectra of cross-linked

FTIR analysis

The FT-IR spectra of MMt-Na^+, cross-linked (TPGDA)/MMt-Li^+, cross-linked (TPGDA)/MMt-Na^+ andcross-linked (TPGDA)/MMt-K^+ are represented in Fig.4 (a, b, c and d) respectively. The band located at 3640 cm^{-1}corresponds to OH stretching Al-OH. The band located at 3450 cm^{-1}characterizes the deformation vibrations of H_2O (Madejová, 2003). As well as the band of 1640 $cm^{-1}$is attributed to the vibrations of O-H of the adsorbed water. The intense band centered at 1050 cm^{-1} corresponds to the valence vibrations

2014). The absorption band at approximately 1715cm^{-1} reflected the stretching vibration of the C=O group and the absence of the characteristic band of the CH_2=C bond, which confirms the radical polymerization of TPGDA.

(TPGDA)/MMt-Li$^+$nanocomposite, cross-linked (TPGDA)/MMt-Na$^+$ nanocomposite and cross-linked (TPGDA)/MMt-K$^+$. The bandsaround 2974 and 2863cm^{-1} have been allocated to the asymmetric stretch and symmetrical stretch vibrations of the –CH_2 group of TPGDA (Wu et al.,

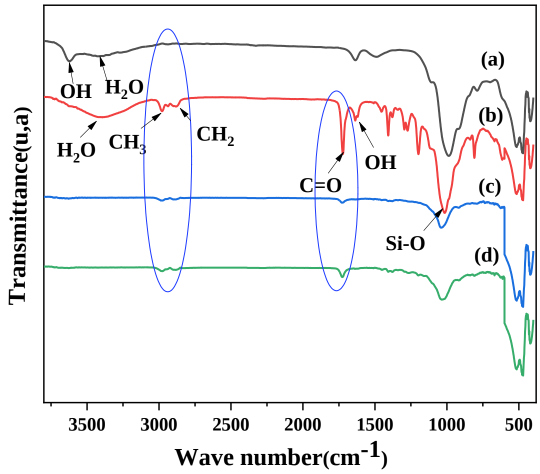

Fig. 4 FTIR spectra of : (a) MMt-Na$^+$, (b) cross-linked (TPGDA)/MMt-Li$^+$ nanocomposite, (c) cross-linked (TPGDA)/MMt-Na$^+$ nanocompositeand (d) cross-linked (TPGDA)/MMt-K$^+$nanocomposite.

montmorillonite. The speed of this transformation reaches its peak at 122°C. Stages 2: loss in weight of 1% and the speed of transformation gets to its peak at 475°C.Stages 3:loss in weight of 5%. The speed of transformation reaches its peak at 649°C(Yılmaz et al., 2013). This is the result of the removal of hydroxylfrom the structure of the montmorillonite.

Thermal analysis of cross-linked (TPGDA)/MMt–M$^+$ nanocomposites 1408

The DTG-TGA curves of the montmorillonite purified are shown in (Fig.5). For the weight loss curve and the differentiation of proportional weight variation, we noticed three stages of the weight loss process:-Stage 1: weight loss of 9% due to the elimination of the water of salvation(Bujdák et al., 1994), without modification of the crystal structure of the

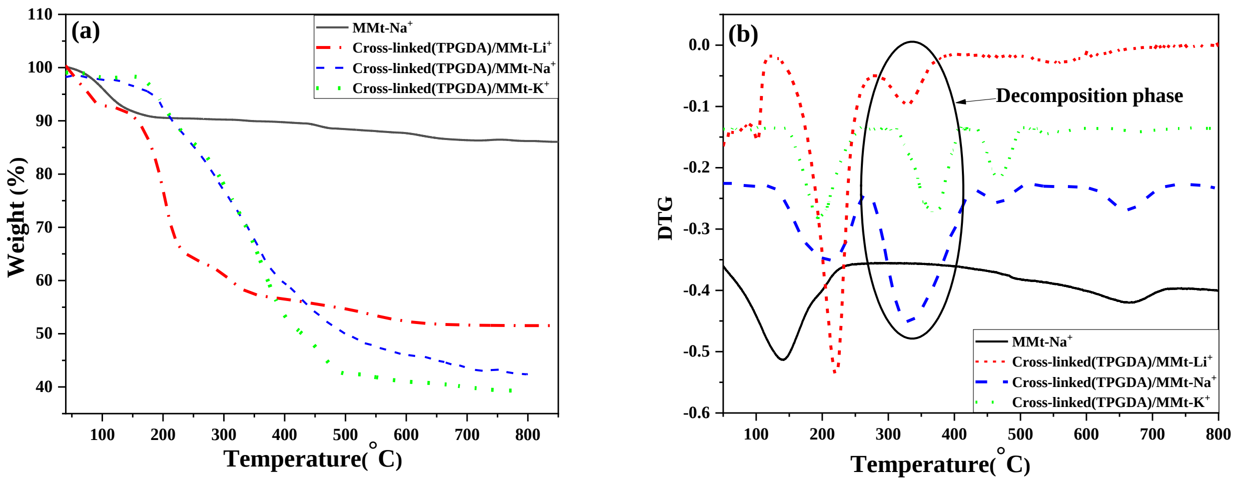

Fig. 5(a) TG curves of MMt-purified and cross-linked (TPGDA)/MMt-M^+nanocomposite and (b) DTG curves of MMt-purified and cross-linked (TPGDA)/MMt-M^+nanocomposite .

The TGA-DTG spectra of cross-linked (TPGDA)/MMt-Li^+,cross-linked (TPGDA)/MMt-Na^+ andcross-linked(TPGDA)/MMt-K^+nanocomposites are presented in the (Fig. 5).The TGA curves showed the thermal stability of all nanocomposite materials and this before 200°C. The total weight loss during the thermogravimetric analysis of the nanocomposites presents several zones: the first zone of 129°C to 280°C corresponds to the evaporation of water. A second zone of weight loss between (280-440°C) due to the decomposition of cross-linked (TPGDA) inside the inter-foliar space of montmorillonite. An inflection is also observed in the region of the temperature range (500-900°C) due to the destruction and recrystallization of the silicate network. These zones are associated with three thermal phenomena observed according to the DTG curves, the endothermic phenomena from (190 to 280°C), between (450-600°C) correspond to the dehydration and dehydroxylation of montmorillonite and (300-450°C) correspond to the oxidation of organic matter. The ranges of the weight loss regions and the corresponding peak temperatures are given in table (2).

Table 2.TG/DTG Analysis of montmorillonite purified and the nanocomposite samples

Data	MMt- purified	cross-linked (TPGDA)/MMt-Li^+	cross-linked (TPGDA)/MMt-Na^+	Crosslinked (TPGDA)/MMt-K^+
Temp. interval and (peak temp.) (ıC), I. Region Weight loss (%), I. Region	100–280 (122) 9	200–280 (220) 33.04	200–280 (214) 16.68	190–280 (192) 14.34
Temp. interval and (peak temp.) (ıC), II. Region Weight loss (%), II. Region	400–560 (475) 1	280-400 (328) 8.71	280-400 (335) 25.42	280-400 (368) 33.1
Temp. interval and (peak temp.) (ıC), III. Region Weight loss (%), III. Region	560–720 (649) 5	400-550 (549) 5.85	400-550 (470) 7.21	400-500 (467) 9.44

Temp. interval and (peak temp.) (ıC), IV. Region Weight loss (%), IV. Region			630–700 (667) 5.77	600–700 (679) 3.03

This can be linked to thermodynamic parameters (ΔH, ΔG) that are calculated using TGA data, with positive values indicating that the process is non-spontaneous. To determine the kinetics parameters, a modified version of the Coats and Redfern model described in Equation (1) was utilized.

$$\log\left[\frac{-\log(1-\alpha)}{T^2}\right]=\log\frac{AR}{\beta E_a}\left[1-\frac{2RT}{E_a}\right]-\frac{E_a}{2.303RT} \quad ....(1)$$

Where*A* is pre-exponential factor, β is heating rate (10 C/min), *R* is general gas constant (8.3143 $Jmol^{-1}\,K^{-1}$), *Ea* is activation energy and *T* is temperature (K). By constructing graphs of *ln[ln(1 - x)]* versus *1000/T* for decomposition phase, as shown in (Fig.6), the activation energy values were determined. Subsequently, additional parameters were calculated using fundamental thermodynamic equations, similar to the approach employed in previous papers (Al-Bayatyet al, 2020; Moussout et al, 2018).

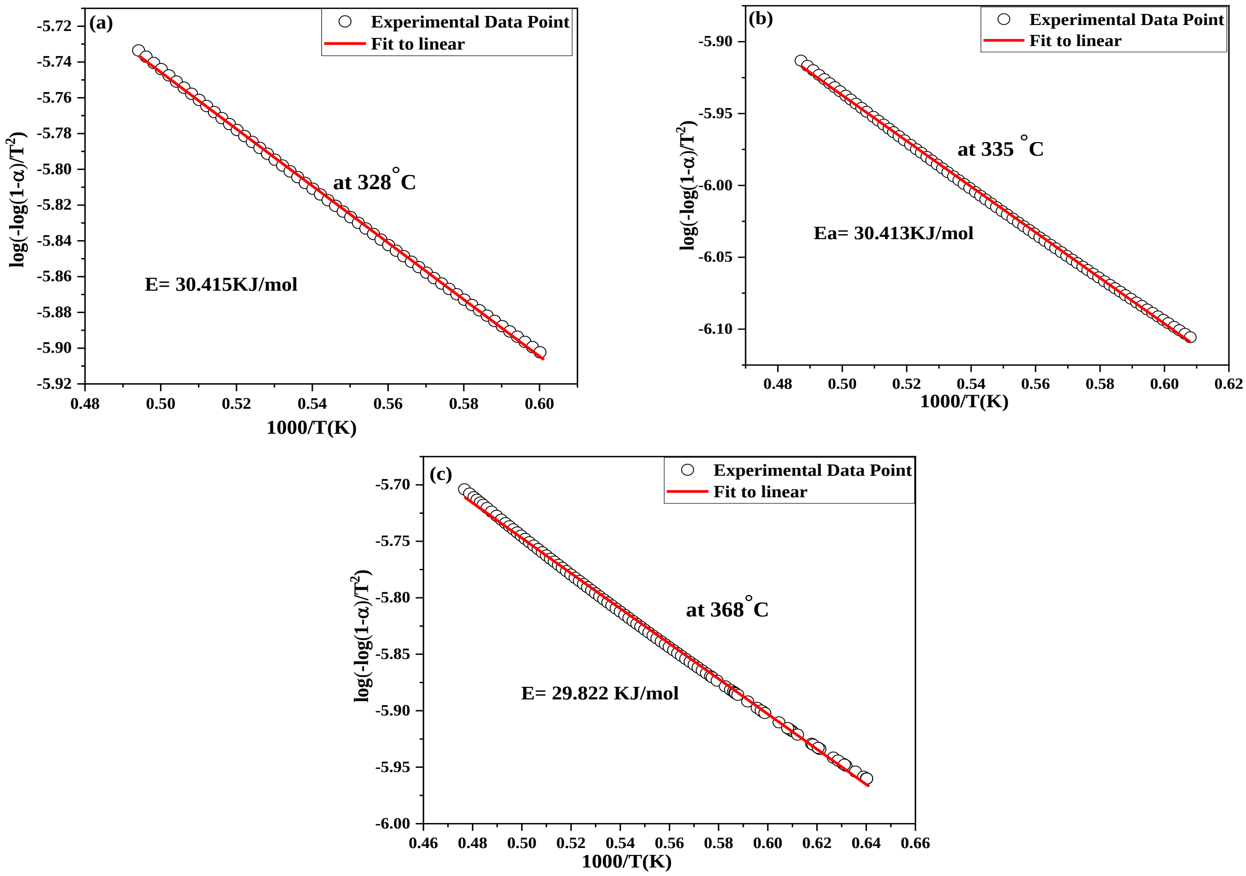

Fig. 6.Plot of [log(-log(1-)/T^2)]vs 1000/T of Decomposition phase: (a) cross-linked (TPGDA)/MMt-Li^+nanocomposite, (b) cross-linke (TPGDA)/MMt-Na^+nanocomposite and (c) cross-linked (TPGDA)/MMt-K^+nanocomposite.

The resulting values for each phase, presented in (Table 3), demonstrated those decomposition phases are characterized by a non-spontaneous nature.

Table 3. Kinetic and thermodynamic parameters of decomposition phase during thermogravimetric analysis of uncalcinedcross-linked (TPGDA)/MMt-M^+ nanocomposite.

cross linked (TPGDA)/MMt-M^+ nanocomposite	Temp (K)	Ea ($kJmol^{-1}$)	ΔH ($Jmol^{-1}K^{-1}$)	ΔS ($Jmol^{-1}K^{-1}$)	ΔG ($Jmol^{-1}$)
Li^+	601	30.415374	-4966.48	-310.953	181916.2
Na^+	608	30.419202	-5024.67	-318.782	188795.2
K^+	641	29.822034	-5299.64	-321.717	200921.3

montmorilloniteis activated by K^+ cation (Fig.6d), for this compound some unaggregated particles can be seen, their seizes are less than 1µm. Moreover, the XRD analysis proves the insertion of cations and TPGDA in the inter-foliar space, the SEM images prove also their adsorption on the montmorillonite external surfaces which conclude that the mixing of the montmorillonite, cations and TPGDA is controlled by the insertion in the inter-foliar space and adsorption.

SEM analysis

The SEM images of the synthesized nanocomposites are illustrated in (Fig.7), all images prove the granular form of the montmorillonite, with a strong tendency for aggregation, the aggregation is well seen on the (Fig.6a), clusters larger than 10 µm without uniform shape are observed, the aggregation is decreased when the cations and TPGDA are added, the weak one is observed when the

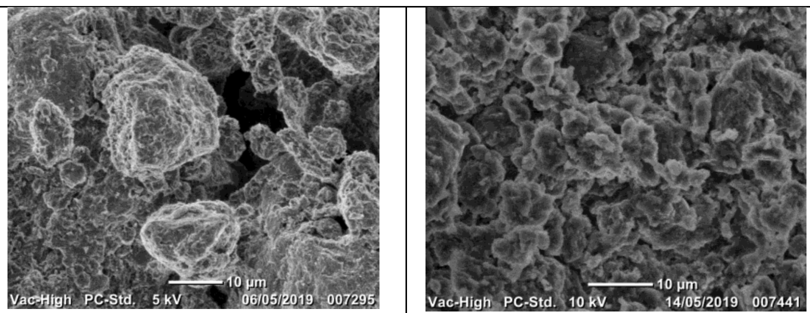

(A) (B)

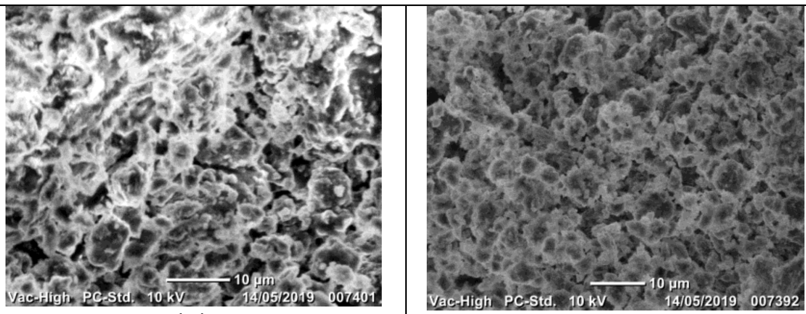

(C) (D)

Fig. 7SEM images of (A) MMt-purified, (B) cross-linked (TPGDA)/MMt-Li^{+} nanocomposite, (C) cross-linked(TPGDA)/MMt-Na^{+} nanocomposite and (D) cross-linked (TPGDA)/MMt- K^{+} nanocomposite.

11.82 of the cross-linked (TPGDA)/MMt-Na^{+}nanocomposite. While the particle size dispersion of cross-linked (TPGDA)/MMt-Li^{+}nanocomposite indicates the presence of a group of particles smaller between 7 and 12 microns. The highest dispersion was (~90%) by particles of 11.82µm. Less dispersion (~10%) involving particles of 7.02 µm. The particles have arithmetic mean diameter, the median particle size of 9.35, 9.23 respectively. The biggest particle size in the case of the composite may be attributed to the formation of intercalation. However, the possibility of clay particles being aggregated to a bigger size and the clay encapsulating these polymer particles cannot also be ignored.

Particle Size Analysis

Fig.8(a, b, c) shows the particle size distribution of cross-linked (TPGDA)/MMt-Li^{+}nanocomposite, cross-linked (TPGDA)/MMt-Na^{+} nanocomposite and cross linked (TPGDA)/MMt-K^{+} nanocomposite. The particle-sizedispersion of cross linked (TPGDA)/MMt-Na^{+} and cross-linked (TPGDA)/MMt-K^{+} nanocomposite indicates the existence of particles assortment of sizes interchanging between 9 and 16µm. The highest dispersion (~90%) is produced by particles of 15.91µm.This population complements through a lesser collection (~10 %) which involves particles of 9.06µm. The particles has arithmetic mean diameter, the median particle size of ~19.22, 11.64 respectively of the cross-linked (TPGDA)/MMt-K^{+} nanocomposite and 20.35,

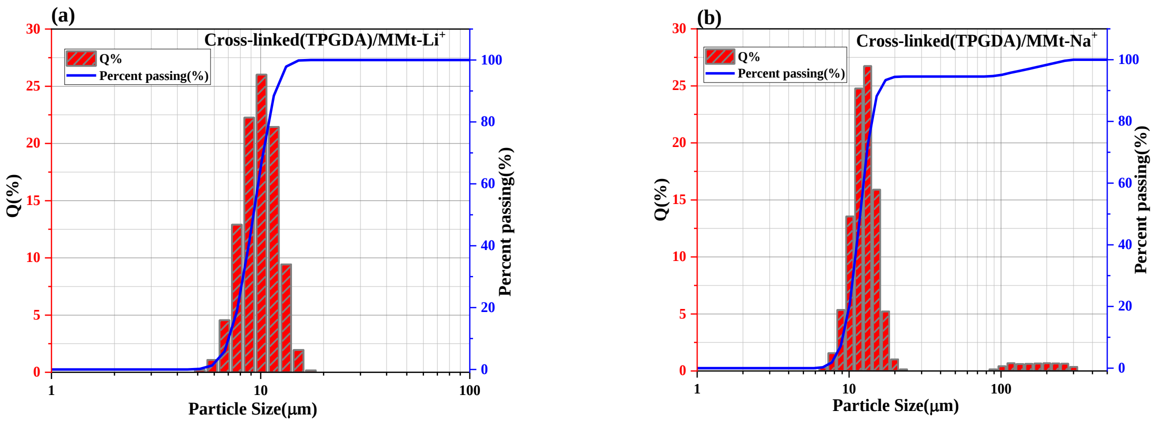

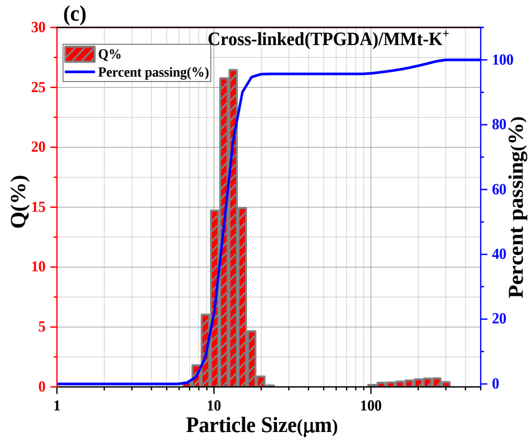

Fig. 8 Particle size distribution of the: (a) cross-linked (TPGDA)/MMt-Li+ nanocomposite, (b) cross-linke(TPGDA)/MMt-Na+ nanocomposite and (c) cross-linked (TPGDA)/MMt-K+ nanocomposite.

ACKNOWLEDGMENT

The samples were meticulously prepared in the physics laboratory located at MabroukiNouari in DjebelMessaad, M'sila, Algeria. The measurements of XRD were conducted with invaluable assistance from FoudilSahnoune, who is affiliated with the Physics Laboratory in the Department of Physics at the Faculty of Science, University of M'sila, Algeria. Additionally, the implementation of TGA, SEM and FT-IR was made possible thanks to the expertise of HakimaAit Youssef from the Emerging Materials Unit at the University of Setif, Setif, Algeria. The authors would like to express their utmost gratitude to the reviewers for their invaluable comments and suggestions, which greatly enhanced the quality of this work.

Conflict of Interest and Authorship Conformation Form

- All authors have participated in (a) conception and design, or analysis and interpretation of the data; (b) drafting the article or revising it critically for important intellectual content; and (c) approval of the final version.
- This manuscript has not been submitted to, nor is under review at, another journal or other publishing venue.

4. CONCLUSION

In view of all these results, The XRD analysis allowed us to really confirm the intercalation of themontmorillonite layers by (TPGDA) with the displacement of the main line of the d_{001} plane towards the small Bragg angles. Values are ordered as follows:

d_{001}(cross-linked(TPGDA)/MMt-Li^+>d_{001}(cross-linked(TPGDA)/MMt-Na^+)>d_{001}(cross-linked (TPGDA)/MMt-K^+).

FTIR shows, in fact, the appearance of new absorption bands in the sheets of montmorillonite attributed to the molecules of the surfactant used and the decrease in the amount of water. Observation by SEM on the samples allows us to conclude more precisely on their structure and on their homogeneity. The change in particle shape due to the effect of the clay organophilization. The pictures obtained are in good agreement with the results from X-ray diffraction. The thermal analysis confirms that the intercalation tokes place by the presence of new peaks attributed to the TPGDA to the different cations of the surfactants. It is noted that the modification of the homoionic-montmorillonite tends to limit the presence of water and that the modification conditions cause variations in the amount of water in the montmorillonite. The thermal stability of cross-linked (TPGDA)/MMt-M^+ nanocomposite is greater than that of montmorillonite purified.

ABS/montmorillonitenanocomposite. *Applied Clay Science, 25(1-2)*, 49-55. https://doi.org/10.1016/j.clay.2003.08.003

Wan, M., & Li, J. (1998). Synthesis and electrical–magnetic properties of polyaniline composites. *Journal of Polymer Science Part A: Polymer Chemistry, 36(15)*, 2799-2805. https://doi.org/10.1002/(SICI)1099-0518(19981115)36:15<2799::AID-POLA17>3.0.CO;2-1

Zheng, W., Wong, S. C., & Sue, H. J. (2002). Transport behavior of PMMA/expanded graphite nanocomposites. *Polymer, 43(25)*, 6767-6773. https://doi.org/10.1016/S0032-3861(02)00599-2

Barnakov, Y. A., Scott, B. L., Golub, V., Kelly, L., Reddy, V., & Stokes, K. L. (2004). Spectral dependence of Faraday rotation in magnetite-polymer nanocomposites. *Journal of Physics and Chemistry of Solids, 65(5)*, 1005-1010.https://doi.org/10.1016/j.jpcs.2003.10.070

Wan, M., & Fan, J. (1998). Synthesis and ferromagnetic properties of composites of a water soluble polyaniline copolymer containing iron oxide. *Journal of Polymer Science Part A: Polymer Chemistry, 36(15)*, 2749-2755.https://doi.org/10.1002/(SICI)1099-0518(19981115)36:15<2749::AID-POLA11>3.0.CO;2-O

Madejová, J., Arvaiová, B., &Komadel, P. (1999). FTIR spectroscopic characterization of thermally treated Cu^{2+}, Cd^{2+}, and Li^{+}montmorillonites. *SpectrochimicaActa Part A: Molecular and Biomolecular Spectroscopy, 55(12)*, 2467-2476.https://doi.org/10.1016/S1386-1425(99)00039-6

Tyagi, B., Chudasama, C. D., &Jasra, R. V. (2006). Determination of structural modification in acid activated montmorillonite clay by FT-IR spectroscopy. *SpectrochimicaActa Part A: Molecular and Biomolecular Spectroscopy, 64(2)*, 273-278.https://doi.org/10.1016/j.saa.2005.07.018

Kubranová, M., Jóna, E., Rudinská, E., Nemceková, K., Ondrušová, D., &Pajtášová, M. (2003). Thermal properties of Co-, Ni-and Cu-exchanged montmorillonite with 3-hydroxypyridine. *Journal of thermal analysis and calorimetry, 74(1)*, 251-257.https://doi.org/10.1023/A:1026350424642

- The authors have no affiliation with any organization with a direct or indirect financial interest in the subject matter discussed in the manuscript

REFERENCES

Picard, E., Vermogen, A., Gérard, J. F., &Espuche, E.(2007). Barrier properties of nylon 6-montmorillonite nanocomposite membranes prepared by melt blending: Influence of the clay content and dispersion state: Consequences on modelling. *Journal of Membrane Science*, *292(1-2)*, 133-144. https://doi.org/10.1016/j.memsci.2007.01.030

Ogasawara, T., Ishida, Y., Ishikawa, T., Aoki, T., & Ogura, T. (2006). Helium gas permeability of montmorillonite/epoxy nanocomposites. *Composites Part A: Applied Science and Manufacturing, 37(12),* 2236-2240. https://doi.org/10.1016/j.compositesa.2006.02.015

Sheldon, R. P. (1982). Composite polymeric materials.

Alexandre, M., & Dubois, P. (2000). Polymer-layered silicate nanocomposites: preparation, properties and uses of a new class of materials. *Materials science and engineering: R: Reports, 28(1-2)*, 1-63.https://doi.org/10.1016/S0927-796X(00)00012-7

Okada, A., &Usuki, A. (1995). The chemistry of polymer-clay hybrids. *Materials Science and Engineering: C, 3(2)*, 109-115.https://doi.org/10.1016/0928-4931(95)00110-7

Reynaud, E., Jouen, T., Gauthier, C., Vigier, G., & Varlet, J. (2001). Nanofillers in polymeric matrix: a study on silica reinforced PA6. *Polymer, 42(21)*, 8759-8768. https://doi.org/10.1016/S0032-3861(01)00446-3

Yang, F., & Nelson, G. L. (2004). PMMA/silica nanocomposite studies: synthesis and properties. *Journal of applied polymer science, 91(6)*, 3844-3850. https://doi.org/10.1002/app.13573

Gilman, J. W. (1999). Flammability and thermal stability studies of polymer layered-silicate (clay) nanocomposites. *Applied clay science, 15(1-2)*, 31-49.https://doi.org/10.1016/S0169-1317(99)00019-8

Wang, S., Hu, Y., Zong, R., Tang, Y., Chen, Z., & Fan, W. (2004). Preparation and characterization of flame retardant

830.https://doi.org/10.1016/j.jhazmat.2009.04.022

Wu, L., Yang, C., Mei, L., Qin, F., Liao, L., &Lv, G. (2014). Microstructure of different chain length ionic liquids intercalated into montmorillonite: a molecular dynamics study. *Applied clay science, 99*, 266-274. https://doi.org/10.1016/j.clay.2014.07.004

Bujdák, J., &Slosiariková, H. (1994). Dehydration and dehydroxylation of reduced charge montmorillonite. *Journal of Thermal Analysis and Calorimetry,41(4)*, 825-831.https://doi.org/10.1007/bf02547162

Yılmaz, M. S., Kalpaklı, Y., &Pişkin, S. (2013). Thermal behavior and dehydroxylation kinetics of naturally occurring sepiolite and bentonite. *Journal of thermal analysis and calorimetry, 114(3)*, 1191-1199. https://doi.org/10.1007/s10973-013-3152-x

Al-Bayaty, S. A., Al-Uqaily, R. A., &Jubier, N. J. (2020). Using the Coats-Redfern method during thermogravimetric analysis and differential scanning calorimetry analysis of the thermal stability of epoxy and epoxy/silica nanoparticle nanocomposites. *Journal of Southwest Jiaotong University, 55(4)*. https://doi.org/10.35741/issn.0258-2724.55.4.2

Moussout, H., Ahlafi, H., Aazza, M., &Sekkate, C. (2018). Kinetic and mechanism studies of the isothermal degradation of local chitin, chitosan and its biocompositebentonite/chitosan. *Cellulose, 25*, 5593-5609.https://doi.org/10.13171/mjc.2.3.2013.22.01.20

Z. Radojevic, A. Mitrovic, *Journal of the European Ceramic Society, 27* (2007) 1691–1695. https://doi.org/10.1016/j.jeurceramsoc.2006.04.152

Haouzi, A., Kharroubi, M., Belarbi, H., Devautour-Vinot, S., Henn, F., &Giuntini, J. C. (2004). Activation energy for dc conductivity in dehydrated alkali metal-exchanged montmorillonites:experimental results and model. *Applied clay science, 27(1-2)*, 67-74.https://doi.org/10.1016/j.clay.2003.12.024

Berend, I. (1991). Les mécanismes d'hydratation de montmorillonites homoioniques pour des pressions relatives inferieures à 0.95 (Doctoral dissertation, Institut National Polytechnique de Lorraine).

Madejová, J. (2003). FTIR techniques in clay mineral studies. *Vibrational spectroscopy, 31(1)*, 1-10. https://doi.org/10.1016/S0924-2031(02)00065-6

dos Santos, V. C. G., Grassi, M. T., & Abate, G. (2015). Sorption of Hg (II) by modified K10 montmorillonite: influence of pH, ionic strength and the treatment with different cations. *Geoderma, 237*, 129-136. https://doi.org/10.1016/j.geoderma.2014.08.018

Sposito, G., Prost, R., &Gaultier, J. P. (1983). Infrared spectroscopic study of adsorbed water on reduced-charge Na/Li-montmorillonites. *Clays and clay minerals, 31(1)*, 9-16.https://doi.org/10.1346/CCMN.1983.0310102

Wu, P., Wu, W., Li, S., Xing, N., Zhu, N., Li, P.,& Dang, Z. (2009). Removal of Cd^{2+} from aqueous solution by adsorption using Fe-montmorillonite. *Journal of Hazardous Materials, 169(1-3)*, 824-